

# First principles study of Li intercalated carbon nanotube ropes

Jijun Zhao <sup>a\*</sup>, Alper Buldum <sup>a</sup>, Jie Han <sup>b</sup>, Jian Ping Lu <sup>a †</sup>

<sup>a</sup>: *Department of Physics and Astronomy, University of North Carolina at Chapel Hill, Chapel Hill, NC 27599*

<sup>b</sup>: *NASA Ames Research Center, Mail Stop T27A-1, Moffett Field, CA 94035*

(September 24, 2018)

## Abstract

We studied Li intercalated carbon nanotube ropes by using first principles methods. Our results show charge transfer between Li and C and small structural deformation of nanotube due to intercalation. Both inside of nanotube and the interstitial space are susceptible for intercalation. The Li intercalation potential of SWNT rope is comparable to that of graphite and almost independent of Li density up to around  $\text{LiC}_2$ , as observed in recent experiments. This density is significantly higher than that of Li intercalated graphite, making nanorope to be a promising candidate for anode material in battery applications.

71.20.Tx, 61.48.+c, 71.15.Pd, 68.65.+g

arXiv:cond-mat/9910143v2 28 Jan 2000

Carbon nanotubes are currently attracting interest as constituents of novel nanoscale materials and device applications [1–3]. Novel mechanic, electronic, magnetic [2] and chemical properties [3] in these one-dimensional materials have been discovered. Single-walled nanotubes (SWNTs) form nanorope bundles with close-packed two-dimensional triangular lattices [4]. These rope crystallites might offer an all-carbon host lattice for intercalation and energy storage. On analogy of the Li intercalated graphite [5], carbon nanorope is expected to be a candidate of anode materials for Li-ion battery applications [6]. Recent experiments found much higher Li capacity ( $\text{Li}_{1.6}\text{C}_6$ ) in SWNTs than those of graphite ( $\text{LiC}_6$ ) [7]. The Li capacity can be further improved up to  $\text{Li}_{2.7}\text{C}_6$  after ballmilling the nanotube samples [8]. This high capacity of Li in nanorope implies lower weight and longer life time in the battery applications [9].

First principles calculations have been successfully used to identify the cathode materials for lithium batteries [10]. In previous theoretical works, K-doped small individual carbon nanotubes was studied by first principles electronic structure calculations [11]. Empirical force field model was also employed to simulate K doped SWNT ropes [12]. However, there is no first principles study on the Li-intercalated SWNT ropes. There are lots of open questions such as: (1) what is the maximum Li intercalation density; (2) where the intercalated Li ions sit; (3) what is the nature of interaction between Li and the carbon nanotube; (4) does the intercalation modify the structure of nanotube. In this letter, we present results obtained by first principles SCF pseudopotential calculations. Several model systems of intercalated nanotube bundle are studied and the results are discussed with the available experiments.

In this work, first principles SCF pseudopotential total-energy calculation and structural minimization are carried out within the framework of local-density approximation on a plane-wave basis with an energy cutoff of 35 Ry. The Car-Parrinello algorithm with  $\Gamma$  point approximation is used in the electronic structure minimization [13,14]. The ion-electron interaction is modeled by Troullier-Martin norm-conserving nonlocal pseudopotential [15] in Kleinman-Bylander form [16]. Plane-wave pseudopotential program, CASTEP [17], is used for structural minimization on some selected systems.

## FIGURES

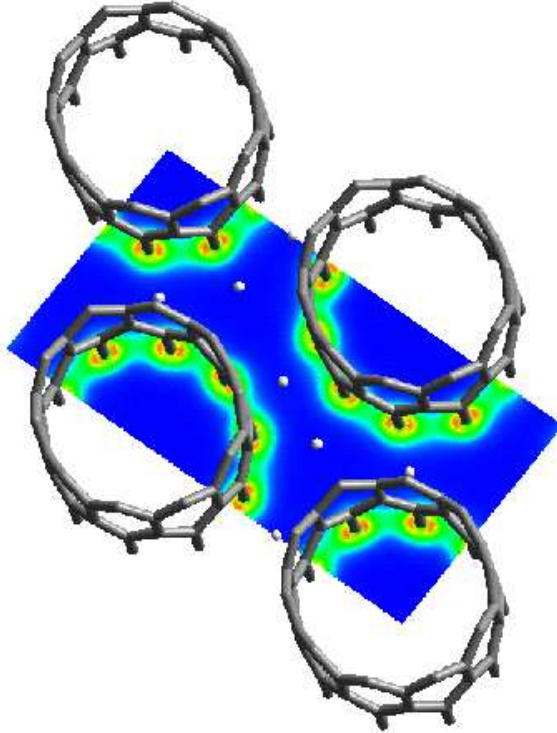
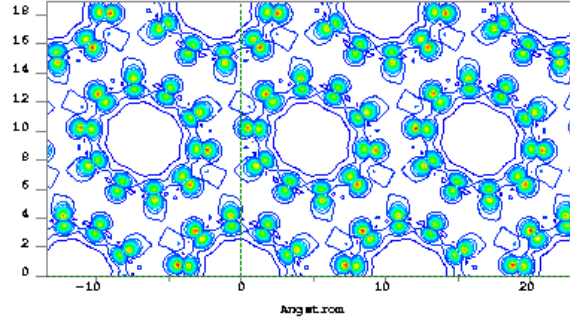


FIG. 1. Geometric structure and total electron density distribution (slice at (100) direction) of relaxed Li intercalated (10,0) tube bundle  $\text{Li}_5\text{C}_{40}$ . Small white balls denote Li atoms. Red, yellow, green, blue colors on the slice indicate electron density from higher and lower. No significant charge density on lithium sites is found, indicating charge transfer between Li and nanotubes.

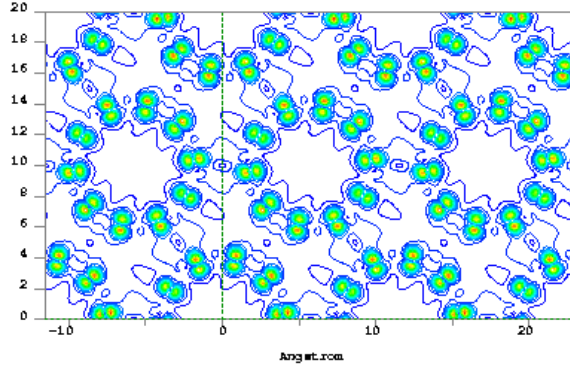
The tube bundle is modeled by an uniform two dimensional hexagonal lattice. The SWNTs studied here include both (10,0), (12,0) zigzag and armchair (8,8), (10,10) tubes. The Li intercalated graphite and bulk Li are also investigated as reference. The initial configuration of Li atoms are assumed to be on high-symmetric sites which maximize the Li-Li distance (see Table II for details).

In Fig.1, we plot the relaxed structure and charge density of (10,0) tube bundle with 5 Li atoms per unit cell. After structural minimization, the Li atoms only slightly shift from their initial symmetric configuration. This shows that symmetry and maximum Li-Li distance are good criteria for choosing Li configuration. The Li intercalation also slightly modifies the shape of carbon nanotubes (see Fig.1 and Fig.2). This result differs from a

previous empirical force field simulation on K doped (10,10) SWNT, in which significant deformation on nanotubes was found [12] (Using the same force field model, we also obtain large deformation). The discrepancy between first principle and empirical calculations demonstrates the importance of quantum effect and the insufficiency of empirical potential in such systems.



(a)



(b)

FIG. 2. Contour plots of the occupied conduction orbital densities near Fermi level (a), and empty orbital densities above Fermi level (b) of (10,0) tube bundle on the (001) plane. Red, yellow, green, blue colors indicate electron density from higher and lower. Conduction orbitals are obviously derived from  $\pi$  bonds between C atoms. In (a), there is very low conduction electron density pass through Li sites; whereas more distinct distributions of empty states are found around Li ions in (b). Both indicate charge transfer between Li and C.

Fig.1 shows that there is almost no total charge density distribution in the space between SWNTs. To further understand the charge distribution, in Fig.2 we present the contour plots of both occupied (a) and empty (b) orbitals near Fermi level. We find the conduction band

orbitals are concentrated on the carbon tubes, while the empty states has some distribution passing through the Li sites. In Fig.3, we compare the band structure near Fermi energy of tube bundle and that of intercalated bundle. Although the individual (10,0) tube and its bundle are all semiconductors, the intercalated tube bundle is found to be metallic. For valence band, only small modification upon intercalation is observed. In contrast, the hybridization between lithium and carbon has significant influence on conduction band and introduces some new states, similar to that found in Ref.[10]. All these analysis show that there is almost complete charge transfer and the conduction electrons mainly occupy the bands originated from carbon nanotubes.

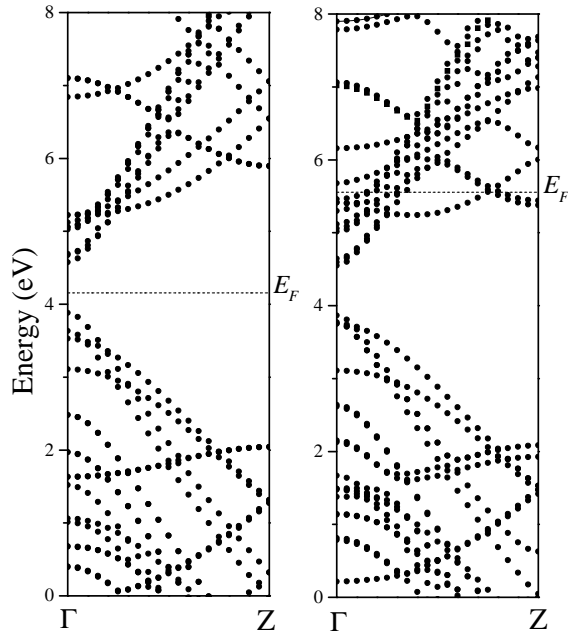


FIG. 3. Electronic band structures of pure (left) and Li intercalated (right) (10,0) tube bundle. Most of the bands are not affected by Li atoms, whereas some new conduction bands are introduced. Most conduction electrons reside on the bands associated with carbon nanotube, indicating charge transfer from Li to nanotube.

Our calculation on other nanotube bundles such as (10,10) tube bundle ( $\text{Li}_5\text{C}_{40}$ ) show similar charge transfer between Li ions and carbon host. The observation of charge transfer

agrees with previous *ab initio* calculation on K doped individual small carbon nanotubes [11]. Similar effect is well known in alkali-metal-doped fullerenes [18]. Experimentally, the charge transfer is supported by Raman [19] and NSR [20] measurements on alkali-metal doped SWNT materials. These suggest that the cohesion between Li and carbon nanotube is mainly ionic. However, we have tried a simple model in which complete charge transfer and uniform charge distribution on C atoms are assumed. Interactions with different screening lengths were tested. We find that this simple model is not sufficient to describe our results, indicating the importance of screening and electron correlations.

To understand where the Li ions can be intercalated, we compare the intercalation energy of two typical Li sites with high symmetry, the center of tube and interstitial site of hexagonal lattice. The total energy and equation of states of the tube bundle are calculated via Car-Parrinello electronic minimization method [14]. The optimal distance between neighboring tubes are then determined. The intercalation energy is obtained by subtracting the energy of the pure nanorope from the total energy of intercalated system. SWNT bundles composed of (10,0), (8,8), (12,0) and (10,10) tubes are studied (Table I). In general, the energy of the Li atoms inside the tube is found to be lower than or comparable to those outside the tube, implying that both the inside and outside of nanotube are favorable for Li intercalation. For smaller tube, the center of tube is less favorable because of the strong core repulse between Li ions and carbon walls.

To study this issue further, we consider nanorope with different intercalation density by putting certain number of lithium atoms at both interstitial sites and those inside the tube. Typical Li configurations are briefly illustrated in Table II. We find that the energies of both the Li sites outside and inside the nanotube are comparable even up to rather high intercalation density. For instance, the energy difference of nine Li ions all inside or outside the (10,10) tube is only 0.36 eV per Li atom. We also find that the intercalation energy is not sensitive to Li arrangements at higher concentration. All these results imply that both inside and outside of the tubes can be simultaneously intercalated to achieve higher Li density.

## TABLES

Table I. The energy  $\Delta E$  (which one Li per unit cell) between the Li reside in interstitial site (a) or at the center of nanotube (c) (see Table II for coordinates). For smaller tube, the interstitial site is preferred while the center is better for larger tube.

Nanotube	(10,0)	(12,0)	(8,8)	(10,10)
Radius ( $\text{\AA}$ )	3.91	4.70	5.42	6.78
$\Delta E$ (eV)	0.24	-0.54	-0.20	-2.20

In recent experiments, the intercalation density of as-prepared SWNTs bundles sample was found as  $\text{Li}_{1.6}\text{C}_6$  [7], and improved up to  $\text{Li}_{2.7}\text{C}_6$  after proper ballmilling [8]. The experimental size of carbon nanotubes is close to that of (10,10) tube. We suggest that the ball-milling process creates defects or breaks the nanotube, allowing the Li ions to intercalate inside of the tube. To understand the experimental intercalation density, we study the intercalated (10,0), (12,0), (10,10) tube bundles with intercalation density from 0 to 28 Li ions per unit cell. Typical Li configurations are given in Table II. The intercalation energy as function of intercalation density for nanoropes is compared with that of graphite in Fig.4. We find that the intercalation energy per carbon atom increases linearly with the intercalation density for different tube bundles up to about  $\text{Li}_{0.6}\text{C}$ . In contrast, the Li intercalation in graphite is already saturated at around  $\text{Li}_{0.35}\text{C}$ . We find that the intercalation potentials defined by taking the derivative of intercalation energy with respect to intercalation density for all tube bundles are almost the same. It is comparable to the intercalation potential of graphite and about 0.1 eV higher than the formation energy of bulk lithium.

Table II. Examples of Li intercalation configurations in our study for (10,10) tube bundle a  $18.0\text{\AA} \times 18.0\text{\AA} \times 2.46\text{\AA}$  hexagonal unit cell. For a given Li concentration, symmetric configuration is chosen to maximize the Li-Li distance. a-f are the site indexes and the number in the bracket is their degeneracy. a,b,e sites are outside the tube and c,d,f are inside. x,y,z denote fractional coordinates based on hexagonal lattice of nanorope. N is the Li number in unit cell which contains 40 carbon atoms. X means there is a Li atom on the site while O means no.

Site	a (2)	b (3)	c (1)	d (8)	e (6)	f(4)
x	0.333	0.5	0	0.278	0.278	0.096
y	0.667	0.5	0	0	0.556	0.131
z	0.5	0	0	0	0.50	0.5
N=2	X	O	O	O	O	O
N=3	X	O	X	O	O	O
N=5	X	X	O	O	O	O
N=6	X	X	X	O	O	O
N=13	X	X	O	X	O	O
N=20	O	X	X	X	X	O
N=24	X	X	X	X	X	X

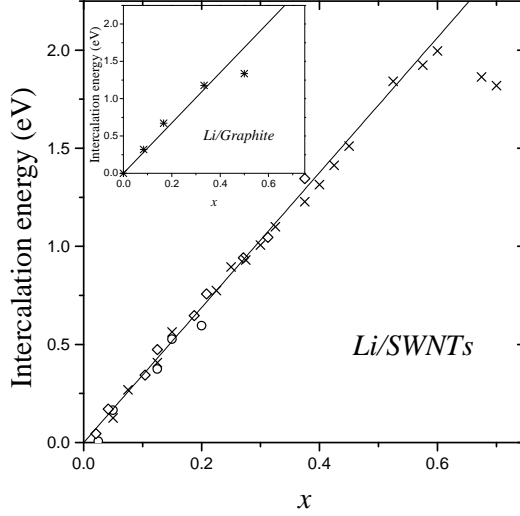


FIG. 4. Intercalation energy per carbon atom as a function of intercalation density,  $x$ , of  $\text{Li}_x\text{C}$  systems. The insert figure show intercalation energy for graphite. Crosses – (10,10) tube bundle; open squares – (12,0) tube bundle; open circles – (10,0) tube bundle. Solid lines are linear fits of the data up to saturation density,  $\text{Li}_{0.6}\text{C}$  for nanorope and  $\text{Li}_{0.35}\text{C}$  for graphite.

From above results, we conclude that the nanorope has a higher capacity for hosting the Li atoms if Li can penetrate into inside space of nanotube. This agrees with the experimental finding that the intercalation density in the ball-milled SWNT bundles can reach up to  $\text{Li}_{2.7}\text{C}_6$ , much higher than  $\text{LiC}_6$  in graphite [7]. The nature of higher Li capacity in nanotube can be related to the low carbon density in nanotube bundle. For example, the average atomic volume for carbon in (10,10) tube bundle is about 60% larger than that of graphite. The calculated saturation intercalation density is also about 60% higher in (10,10) tube bundle than graphite. Additional understanding of high Li concentration can be gained by examine the work function (WF) of nanotube. Although we are unaware of any experimental measurements of WF on SWNT one might expects that its WF to be close to that of  $\text{C}_{60}$  thin films (4.85 eV) [21] and higher than WF of graphite (4.44 eV) [22]. Thus, the electron

in nanorope has lower energy than those in graphite.

In summary, we have performed first principles calculations on the total energy and electronic structures of Li intercalated SWNT nanoropes. The main conclusions are: (1) almost complete charge transfer occurs between Li atoms and SWNTs; (2) the deformation of nanotube structure after intercalation is relatively small; (3) energetically inside of tube is as favorable as interstitial sites for intercalation; (4) the intercalation potential of Li/SWNT is comparable to the formation energy of bulk Li and independent of Li density up to about  $\text{Li}_{0.5}\text{C}$ ; (5) the intercalation density of SWNT bundle is significant high than that of graphite. These results suggest that nanorope is a promising candidate material for anode in battery application.

This work is supported by the U.S. Army Research Office Grant No. DAAG55-98-1-0298, the Office of Naval Research Grant No. N00014-98-1-0597 and NASA Ames Research Center. The authors thank Dr. O.Zhou and Mr. B.Gao for helpful discussions. We gratefully acknowledge computational support from the North Carolina Supercomputer Center.

\*: zhaoj@physics.unc.edu

†: jpl@physics.unc.edu

## REFERENCES

- [1] M.S.Dresselhaus, G.Dressehaus, P.C.Eklund, *Science of Fullerenes and Carbon Nanotubes*, Academic Press, New York, 1996; T.Ebbesen ed., *Carbon Nanotube: Preparation and Properties*, CRC Press, Boca Raton, 1997; R.Saito, G.Dressehaus, M.S.Dresselhaus, *Physics Properties of Carbon Nanotubes*, World Scientific, New York, 1998.
- [2] J.P.Lu, J.Han, *Inter.J.High Electronics and System* **9**, 101(1998).
- [3] P.M.Ajayan, *Chem.Rev.***99**, 1787(1999).
- [4] A.Thess, R.Lee, P.Nikdaev, H.Dai, P.Petit, J.Robert, C.Xu, Y.H.Lee, S.G.Kim, A.G.Rinzler, D.T.Colbert, G.E.Scuseria, D.Tomanek, J.E.Fischer, and R.E.Smalley, *Science***273**, 483(1996).
- [5] M.S.Dresselhaus and G.Dresselhaus, *Adv.Phys.***30**, 1399(1981).
- [6] M.Winter, J.O.Besenhard, M.E.Spahr, and P.Novak, *Adv.Mater.***10**, 7259(1998).
- [7] B.Gao, A.Kleinhammes, X.P.Tang, C.Bower, L.Fleming, Y.Wu and O.Zhou, *Chem.Phys.Lett.***307**, 153 (1999).
- [8] B.Gao, C.Bower, J.D.Lorentzen, L.Fleming, A.Kleinhammes, X.P.Tang, L.E.McNeil, Y.Wu, O.Zhou, unpublished.
- [9] G.Pistoia Ed., *Li Batteries, New Materials, Developments and Perspectives*, Elsevier, Amsterdam, 1994.
- [10] M.K.Aydinol, A.F.Kohan,  
G.Ceder, K.Cho, J.Joannopoulos, *Phys.Rev.B***56**, 1354(1997); G.Ceder, Y.M.Chiang, D.R.Sadoway, M.K.Aydinol, Y.I.Jang, B.Huang, *Nature***392**, 694(1998).
- [11] Y.Miyamoto, A.Rubio, X.Blase, M.L.Cohen, S.G.Louie, *Phys.Rev.Lett.***74**, 2993(1995).
- [12] G.Gao, T.Gagin, W.A.Goddard III, *Phys.Rev.Lett.***80**, 5556(1998).

- [13] R.Car and M.Parrinello, Phys.Rev.Lett.**55**, 2741(1985).
- [14] G.Galli and A.Pasquarello, in *Computational Simulation in Chemical Physics*, edited by M.P.Allen and D.J.Tildesley, (Kluwer, Academic Publisher, 1993), p.261.
- [15] N.Troullier and J.L.Martins, Solid State Commun.**74**, 13(1990); Phys.Rev.B**43**, 1993(1991). The Troullier-Martin pseudopotential used in this work is generated by the Fhi98PP pseudo potential program: see M.Fuchs, M.Scheffler, Comput.Phys.Commun.**119**, 67(1999).
- [16] L.Kleinman and D.M.Bylander, Phys.Rev.Lett.**48**, 1425(1982).
- [17] CASTEP is an *ab initio* program with plane-wave pseudopotential package distributed by MSI.
- [18] H.Enrenreich and F.Spaepen, Ed., *Solid State Physics*, Vol.48, Academic Press, 1994.
- [19] A.M.Rao, P.C.Eklund, S.Bandow, A.Thess, and R.E.Smalley, Nature**388**, 257(1997).
- [20] A.Kleinhammes, X.P.Tang, Y.Wu, et. al. unpublished.
- [21] N.Sato, Y.Saito, H.Shinohara, Chem.Phys.**162**, 433(1992).
- [22] H.Ago, T.Kugler, F.Cacialli, W.R.Salaneck, M.S.P.Shaffer, A.H.Windle, R.H.Friend, J.Phys.Chem.B**103**, 8116(1999).